PHYSICAL, CHEMICAL, AND THERMAL ANALYSIS OF ELECTROSPUN MEMBRANES OF PORCINE COLLAGEN AND SODIUM HEPARIN FOR USE IN BIOMEDICINE

[1]P. OROZCO, [2]Y. MONTOYA, [3]A. GARCÍA-GARCÍA, [4]J. BUSTAMANTE

[1,2,3] Grupo de Dinámica Cardiovascular, Línea Ingeniería de Tejidos y Protésica Cardiovascular, Universidad Pontificia Bolivariana, Medellín, Colombia
[3,4] Comité de Trabajo de Bioingeniería Cardiovascular, Sociedad Colombiana de Cardiología y Cirugía Cardiovascular, Bogotá, Colombia.
[3]Centro de Investigación en Materiales Avanzados, S.C. (CIMAV), Subsede Monterrey, Av. Alianza Norte 202, Parque PIIT, Apodaca, Nuevo León CP 66628, Mexico
E-mail: paola.orozco@upb.edu.co

Abstract - Techniques such as electrospinning mediated by the generation of an electrostatic field have allowed the development of fibrillar biomaterials at the micro and nanometric scale, characteristics that can be modulated by changes in voltage, flow, polymer concentrations, miscibility, and volumetric ratios.The intrinsic physicochemical and mechanical properties of micro- and nanocomposites allow their application in the biomedical field, either as drug delivery vehicles or biological support structures. The aim of this research was to develop a three-dimensional fibrillar structure composed of polyvinyl alcohol (PVA), porcine collagen, and low-molecular-weight sodium heparin. The electrospun membranes were crosslinked and characterized using scanning electron microscopy (SEM), Fourier transform infrared spectroscopy (FTIR), thermogravimetric analysis (TGA), stress-strain testing, and contact angle measurements. The results demonstrate 3D structures with fibrillar morphology with multiscale heterogeneity. Furthermore, the presence of functional groups such as OH, amides, sulfates, and carboxyls was identified, which demonstrates the interaction of the synthetic polymer, protein, and drug. On the other hand, TGA identified phases of polymer evaporation and degradation. Stress-strain curves showed modulus and yield strength variations depending on the polymer concentration. The contact angle results showed changes in hydrophilicity associated with heterogeneity in fiber diameters. The type of structure developed exhibits dynamic characteristics that could favor biological interactions with recognition of active cellular sites for its application in nanomedicine.

Keywords - Electrospun Membrane, Porcine Collagen, Polyvinyl Alcohol, Sodium Heparin

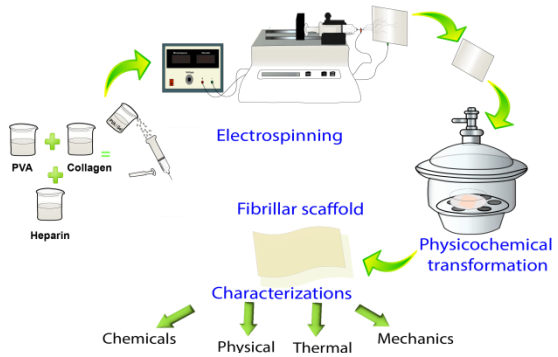


Fig. 1 Electrospinning process, chemical transformation of fibrillar scaffolds of polyvinyl alcohol, porcine collagen, and sodium heparin.

I. INTRODUCCIÓN

The electrospinning technique has allowed the development of biomaterials using synthetic and natural polymers to obtain fibrillar structures at the micro and nanometric scale[1], [2]. The parameters used during the electrospinning process, including the concentration of the polymer solutions, volumetric ratios, flow, voltage, and distance, can influence the morphology and diameters of the fibers [3].Furthermore, these fibrillar structures exhibit a microarchitecture with interconnected pores, seeking to favor cell infiltration, migration, and proliferation processes, for their applications in nanomedicine.[4], [5].

The combination of engineering principles and nanotechnology has allowed to enhance the physical, chemical and biological properties of fibrillar structures through the incorporation of bioactive agents such as drugs, polysaccharides, peptides, nanoparticles, among others, which leads to modifications of the surface area versus volume relationship, around the generation of biomaterials that allow the release of biomolecules through their fibrillar and porous network.[6][7].

In this sense, the intrinsic characteristics of the polymers, as well as the concentrations used in the development of the fibrillar scaffolds, also influence the morphological, hydrophobic or hydrophilic responses, mechanical behaviors and thermal stability.Synthetic polymers used in the development of fibrillar structures include polyethylene oxide (PEO), polylactic-co-glycolic acid (PLGA), poly(L-lactide-co-ε-caprolactone), and polyvinyl alcohol (PVA).[8]. The latter is a hydrophilic, biodegradable, and biocompatible polymer, in addition to providing characteristics such as viscosity and mechanical resistance, which is why it has been used in the development of biomaterials.[9], [10]. However, it

has been reported that biocomposite scaffolds exhibit an increase in the final intrinsic properties of the biomaterial. Therefore, the incorporation of an additional component, such as natural polymers,for example, chitosan, silk fibroin, alginate, hyaluronic acid, and porcine collagen, is considered, where the collagen protein exhibits biocompatibility, biodegradability, and low antigenic effect, properties that make this an ideal polymer for incorporation in the development of biomaterials.[11].

Based on the foregoing, this research was based on the physical, chemical, and thermal analysis using advanced characterization techniques of scaffolds composed of polyvinyl alcohol, porcine collagen, and sodium heparin developed by the electrospinning technique, to obtain a three-dimensional fibrillar structure with micro and nanometric scale characteristics that allow its application in biomedicine.

II. DETAILS EXPERMIENTAL

2.1Manufacturing and crosslinking of electrospun scaffolds

Electrospinning solutions were prepared from a mixture of 12 % polyvinyl alcohol (PVA) and 20 % porcine collagen. The polymer solution was mixed with sodium heparin at a concentration of 10 U/mL in volumetric ratios of 50:45:5 and 50:30:20 (PVA:Col:Hep). The solution was loaded into a syringe and electrospun at a flow rate of 0.6 mL/h and a voltage of 18 kV. The scaffolds underwent physicochemical transformation processes by crosslinking with 20% glutaraldehyde (GA) vapor for 24 h.

2.2 Scanning electron microscopy

The scaffolds were characterized by scanning electron microscopy at 15 kV (Nova NanoSEM 200) to determine the surface morphology and fiber diameters.

2.3 Analysis by Fourier transform infrared spectroscopy

To identify changes in the functional groups of the electrospun scaffolds, a spectrophotometer with an attenuated reflectance module (Spectrum Two, PerkinElmer) was used in a range of 4000 – 400 $cm^{-1}$with a resolution of 4 cm^{-1}.

2.4 Thermogravimetric analysis (TGA)

Thermal analysis (TGA) was performed using 10 mg of sample with measurements at a temperature of 25 to 600 °C with a heating rate of 10 °C/min in an N_2 atmosphere.

2.5 Contact angle

The contact angle was measured using a goniometer. The method used was to deposit a water droplet on the surface of the membranes measuring 1.5 cm × 1.5 cm.

2.6 Mechanical characterization

The mechanical properties were evaluated using tensile tests using a 1 kN load cell at a strain rate of 10 mm/min at room temperature. Finally, stress-strain curves were obtained.

III. RESULTS AND DISCUSSION

3.1 Morphological analysis of electrospun scaffolds

Fig. 1A shows the micrographs obtained by scanning electron microscopy (SEM) of the electrospun membranes without crosslinking, where the surface morphology is observed with the formation of a three-dimensional structure with the presence of continuous fibers and the absence of pearl-type defects. Using processing with the image J® software, the fiber diameters were obtained for the control scaffolds without heparin (PVA50:Col50), and for the scaffolds functionalized with the drug at 5 % (PVA50:Col:45:Hep45) and 20 % (PVA50:Col:30:Hep20), exhibiting average diameter values of 153.33 nm ± 1, 112.29 ± 3 nm, and 135.55 ± 1 nm, respectively.Compared to control scaffolds, heparin-incorporated scaffolds showed smaller fiber diameters with statistically significant differences. ($p < 0.01$ y $p < 0.05$). These results may be associated with the different volumetric ratios of porcine collagen and heparin used in the manufacture of the scaffold, which would affect factors such as viscosity, charge density, and fiber elongation during the electrospinning process, modifying the fibrillar structure depending on the fiber diameters at the micro and nanoscale.

To favor the structural stability of the scaffolds in aqueous environments, the scaffolds were subjected to physicochemical crosslinking processes with 20 % glutaraldehyde (GA).Figure 1B shows the micrographs of the cross-linked scaffolds, which showed widening and fusion of the fibers forming a mesh, as a result of the reaction between the free amino groups of collagen amino acids, such as lysine or hydroxylysine, and the aldehyde groups of GA.[12].For thePVA50:Col50, PVA50:Col:45:Hep45,and PVA50:Col:30:Hep20 scaffolds fiber diameters (Df)of 153.33 ± 1.2 nm, 112.29 ± 3 nm,and 135.55 ± 1.2 nm were obtained, respectively, with statistically significant differences in relation to the control scaffold of $p < 0.0001$ for PVA50:Col:45:Hep45and$p < 0.001$PVA50:Col:30:Hep20.The above denotes an increase inDf as a function of the increase in the volumetric ratio of heparin, which could be related to a greater presence of sulfate groups.

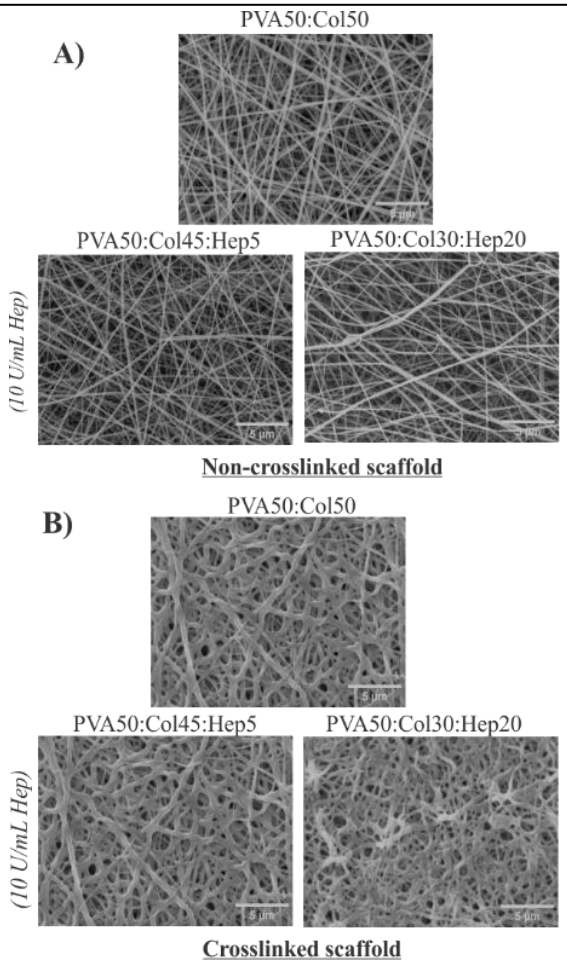


Fig. 1SEM micrographs of PVA-Col-H electrospun scaffolds with and without 10 U/mL. A) Uncrosslinked scaffolds of P50:Col50, P50:Col45:H5,and P50:Col30:H20,and B)Crosslinked scaffolds of P50:Col50, P50:Col45:H5,and P50:Col30:H20. Escala 5 µm.

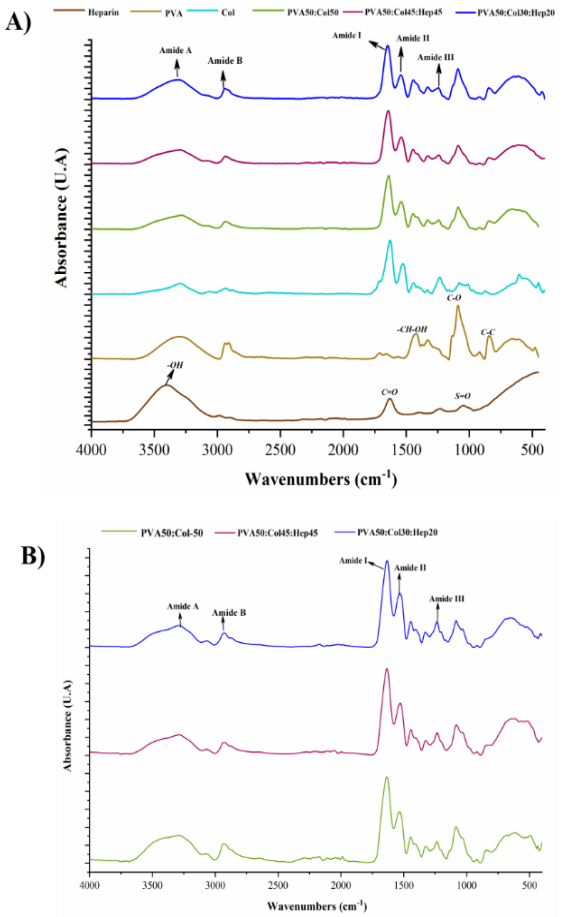


Fig. 2FTIR spectra whereA). PVA, Col-h, and fibrillar matrices PVA50:Col50, PVA50:Col45:H5,and PVA50:Col30:H20 without crosslinking, B) Spectra of crosslinked fibrillar matrices.

3.2 FTIR

In the IR spectra of PVA, a band was identified between 3600 – 3000 cm^{-1} associated with stretching of the O–H groups, peaks at 2940 cm^{-1} and 2910 cm^{-1} due to asymmetric and symmetric stretching of the CH_2 groups, at 1428 cm^{-1} bending of CH and O–H groups, at 1326 cm^{-1} C-O-C vibrations, and at 1090 cm^{-1} C–O stretches(Fig. 2A)[13].

Porcine collagen presented peaks at 3280 cm^{-1} attributed to amide A; 2930 cm-1 for the amide B region; 1630 cm-1 corresponding to amide I; 1530 cm-1 related to amide II; and 1234 cm^{-1} for amide III.For heparin, characteristic peaks were found at wavelengths of 3400 cm^{-1} related toO–H groups, at1630 cm^{-1}, 1400, 1236 to 1044,and 870 cm^{-1}corresponding to O–H, C-H, C=Ostretching, N-Hbending, symmetric and asymmetric S=O stretching, and axial deformation of S=O and C–O–S bonds[14]. Likewise, the scaffolds without and with the incorporation of heparin at 5 % v/v and 20 % v/v were characterized(Fig. 2A), identifying the characteristic vibrational modes of polymers as well as heparin.

Fig. 2B shows the spectra for the crosslinked membranes with no significant differences compared to the uncrosslinked scaffolds.However, taking into account the susceptibility of amide I to interaction with GA, this region was deconvoluted, finding modifications in the secondary structures with transitions in non-crystalline structures (chains (Tyr), Random coils, α-helix, and turns structures) to crystalline structures (sheets andβ turns)[15].

3.3 Thermal analysis

The thermal behavior for the non-crosslinked scaffolds presented three stages of mass loss as a function of time, with temperature ranges between 30 – 150°C (water evaporation), 150 – 350°C (polymer chain degradation), and 350 – 500 °C (carbonyl, oxygen, and sulfate decomposition), respectively.[16]. Furthermore, greater thermal stability was observed in the membranes with 20 % v/v heparin (PVA50:Col30:H20) compared to the other membranes, which could be attributed to the volumetric ratio of the drug incorporated in the scaffold, which favors chemical interactions between sulfate and amino groups(Fig. 3A).

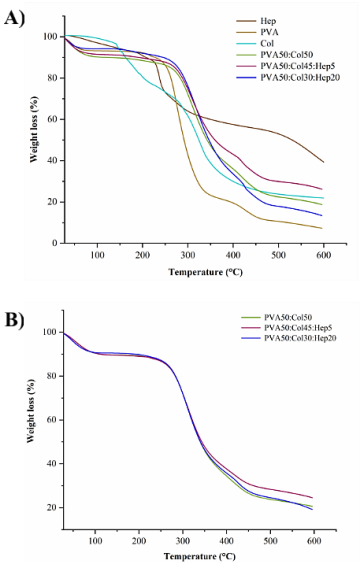


Fig.3TGA curves of electrospun membranes of PVA, porcine collagen, and heparin. A) TGA curves for samples of PVA, Col, heparin, and fibrillar matrices without crosslinking, and B) TGA curves for fibrillar matrices crosslinked.

Fig. 3B shows the thermograms obtained for the cross-linked electrospun membranes. The curves for the three stages of weight loss were identified, where lower mass losses were noted compared to the uncross-linked scaffolds. This is associated with the chemical reactions induced by the cross-linking agent in the secondary structures of porcine collagen[17].

3.4 Contact angle

Electrospun membranes without crosslinking exhibited complete droplet absorption and dissolution of the material from the beginning[18]. While, in the membranes crosslinked with glutaraldehyde vapor, an increase in hydrophobicity was observed with a higher contact angle for the PVA50:Col50, PVA50:Col45:H5, and PVA50:Col30:H20 scaffolds(Fig. 4). These results are attributed to the reorganization of the secondary structures during the crosslinking process, to the concentrations of heparin incorporated in each fibrillar structure, and to the fiber diameters in the scaffolds, where this last characteristic is directly associated with the area-volume ratio and the diffusion of water in the fibers, important factors involved in the development of biomaterials with applications in nanomedicine[19].

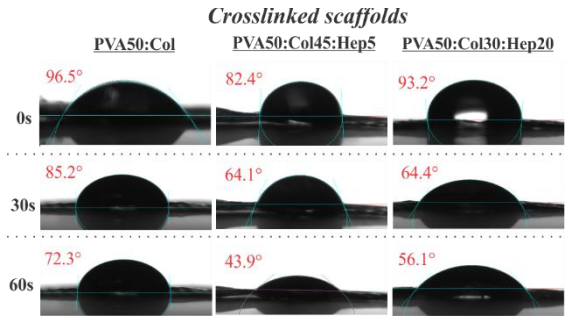


Fig.4Contact angle in the cross-linked fibrillar scaffolds (times 0, 30 and 60 s).

3.5 Mechanical properties

In Fig. 5A, the stress versus strain curves are observed for thePVA50:Col50, PVA50:Col:H45 and PVA50:Col30:H20 membranes without crosslinking, in which a Young's modulus with values of 6.71 ± 1.91 MPa, 8.54 ± 3.12 MPa and 7.81 ± 0.51 was obtained, and values of 0.43 ± 0.14, 0.60 ± 0.08 and 0.60 ± 0.10 for the yield strength respectively, denoting variations in the mechanical properties depending on the proportions of porcine collagen and sodium heparin[10].

On the other hand, lower values for Young's modulus and elastic limit were found in the crosslinked membranes compared to the non-crosslinked scaffolds(Fig.5B). PVA50:Col50 showed a Young's modulus and yield strength of 0.77 ± 0.19 MPa and 0.09 ± 0.00 MPa, PVA50:Col:H45 1.14 ± 0.13 MPa and 0.09 ± 0.02 MPa, andPVA50:Col30:H20 0.39 ± 0.20 MPa and 0.05 ± 0.00 MPa.This behavior is related to the fiber diameters of the scaffolds and the physicochemical modifications caused by crosslinking with GA, modifying the rigidity of the fibrillar micro and nanoarchitecture[20].Likewise, the presence of heparin influences the mechanical behavior due to the affinity and availability of sulfate groups($-SO_3$)that can bind with the amino ($-NH$)and carboxylate(–COO) groups through attractive electrostatic interactions involved in biological processes[21].

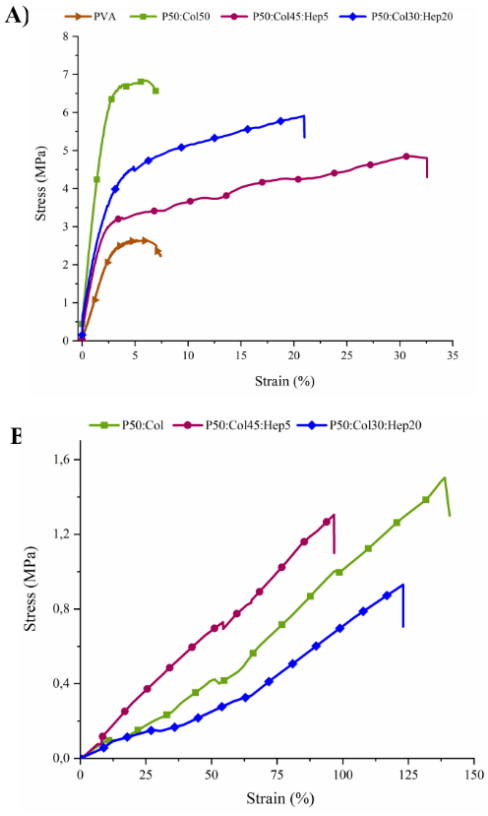


Fig. 5 Stress versus strain curves of fibrillar scaffolds without and with crosslinking: A) fibrillar scaffolds without crosslinking and B) fibrillar scaffolds crosslinked.

IV. CONCLUSION

Using the electrospinning technique, membranes composed of PVA and porcine collagen with the addition of sodium heparin were obtained, which were characterized using physical, chemical, and thermal techniques.

Scanning electron microscopy (SEM) characterization revealed a randomly oriented fibrillar morphology, free of defects, and with fiber diameters on the micro and nanometer scale, which varied depending on the volumetric ratios of the polymers and the drug. The fibrillar structure was crosslinked with an inorganic solvent (glutaraldehyde) to promote structural stability in aqueous environments. This behavior was modulated by the reorganization of the protein's secondary structures, which was validated by Fourier transform infrared spectroscopy.

Contact angle analysis demonstrated that the fibrillar membranes exhibit a hydrophilic surface with angles less than 90°. Likewise, thermogravimetric analysis found an increase in the thermal stability of the scaffolds after the crosslinking process, which varied depending on the volumetric ratios of the natural polymer and sodium heparin, where these generate affinity bonds between functional groups. Furthermore, mechanical tests concluded that the incorporation of porcine collagen and the drug influence the mechanical response of the fibrillar membranes. Finally, the physical, chemical, thermal, and mechanical properties identified in the evaluated fibrillar membranes demonstrated characteristics that allow their application in nanomedicine.

ACKNOWLEDGMENTS

To the Ministry of Science, Technology and Innovation-Minciencias and the Sistema General de Regalías – SGR for scholarship support in the project BPIN2019000100045 (Doctoral Excellence Scholarship Program of the Bicentennial), to grant number BPIN2020000100190 for supportedthis research and the Center for Research in Advanced Materials (CIMAV).

REFERENCES

[1] A. Haider, S. Haider, and I. K. Kang, "A comprehensive review summarizing the effect of electrospinning parameters and potential applications of nanofibers in biomedical and biotechnology," Arab. J. Chem., vol. 11, no. 8, pp. 1165–1188, 2018, doi: 10.1016/j.arabjc.2015.11.015.

[2] S. Anjum et al., "Electrospun Biomimetic Nanofibrous Scaffolds: A Promising Prospect for Bone Tissue Engineering and Regenerative Medicine," Int. J. Mol. Sci., vol. 23, no. 16, 2022, doi: 10.3390/ijms23169206.

[3] E. Hirsch, M. Nacsa, F. Ender, M. Mohai, Z. K. Nagy, and G. J. Marosi, "Preparation and characterization of biocompatible electrospun nanofiber scaffolds," Period. Polytech. Chem. Eng., vol. 62, no. 4, pp. 510–518, 2018, doi: 10.3311/PPch.12854.

[4] P. Domalik-Pyzik and A. Morawska-Chochół, "Preliminary Results on Heparin-Modified Double-Layered PCL and PLA-Based Scaffolds for Tissue Engineering of Small Blood Vessels," J. Funct. Biomater., vol. 13, no. 1, 2022, doi: 10.3390/jfb13010011.

[5] I. Lugoloobi, W. Yuanhao, I. Marriam, J. Hu, M. Tebyetekerwa, and S. Ramakrishna, "Electrospun biomedical nanofibers and their future as intelligent biomaterials," Curr. Opin. Biomed. Eng., vol. 24, no. Figure 1, p. 100418, 2022, doi: 10.1016/j.cobme.2022.100418.

[6] P. Huo, X. Han, W. Zhang, J. Zhang, P. Kumar, and B. Liu, "Electrospun nanofibers of polycaprolactone/collagen as a sustained-release drug delivery system for artemisinin," Pharmaceutics, vol. 13, no. 8, 2021, doi: 10.3390/pharmaceutics13081228.

[7] S. N. Kalva, R. Augustine, A. Al Mamun, Y. B. Dalvi, N. Vijay, and A. Hasan, "Active agents loaded extracellular matrix mimetic electrospun membranes for wound healing applications," J. Drug Deliv. Sci. Technol., vol. 63, no. March, p. 102500, 2021, doi: 10.1016/j.jddst.2021.102500.

[8] A. B. García-Hernández et al., "PVA-Based Electrospun Biomembranes with Hydrolyzed Collagen and Ethanolic Extract of Hypericum perforatum for Potential Use as Wound Dressing: Fabrication and Characterization," Polymers (Basel)., vol. 14, no. 10, 2022, doi: 10.3390/polym14101981.

[9] A. Mhatre, A. Bhagwat, P. Bangde, R. Jain, and P. Dandekar, "Chitosan/gelatin/PVA membranes for mammalian cell culture," Carbohydr. Polym. Technol. Appl., vol. 2, p. 100163, 2021, doi: 10.1016/j.carpta.2021.100163.

[10] M. Sun, Y. Wang, L. Yao, Y. Li, Y. Weng, and D. Qiu, "Fabrication and Characterization of Gelatin/Polyvinyl Alcohol Composite Scaffold," Polymers (Basel)., vol. 14, no. 7, 2022, doi: 10.3390/polym14071400.

[11] A. Pal, A. Kumar Bajpai, and J. Bajpai, "Study on facile designing, swelling properties and structural relationship of gelatin nanoparticles," J. Macromol. Sci. Part A Pure Appl. Chem., vol. 56, no. 3, pp. 206–214, 2019, doi: 10.1080/10601325.2019.1565542.

[12] X. Chen et al., "Fabrication and properties of electrospun collagen tubular scaffold crosslinked by physical and chemical treatments," Polymers (Basel)., vol. 13, no. 5, pp. 1–16, 2021, doi: 10.3390/polym13050755.

[13] C. M. Cholant et al., "Study of the conductivity of solid polymeric electrolyte based on PVA/GA blend with addition of acetic acid," J. Solid State Electrochem., vol. 24, no. 8, pp. 1867–1875, 2020, doi: 10.1007/s10008-020-04605-2.

[14] P. V. A. Bueno et al., "N,N-Dimethyl chitosan/heparin polyelectrolyte complex vehicle for efficient heparin delivery," Int. J. Biol. Macromol., vol. 75, pp. 186–191, 2015, doi: 10.1016/j.ijbiomac.2015.01.030.

[15] F. R. Boroojeni, S. Mashayekhan, and H. A. Abbaszadeh, "The controlled release of dexamethasone sodium phosphate from bioactive electrospun PCL/gelatin nanofiber scaffold," Iran. J. Pharm. Res., vol. 18, no. 1, pp. 111–124, 2019.

[16] S. Kocabay, M. R. Bahar, S. Tekin, R. Akkaya, and B.

Akkaya, "Chemical and biological characterization of sulfated chitosan oligomer as heparin mimics," Polym. Polym. Compos., vol. 29, no. 9_suppl, pp. S1023–S1032, 2021, doi: 10.1177/09673911211035068.

[17] W. Chen, Z. Gao, M. He, Y. Dou, G. Yin, and J. Ding, "Vapor-phase glutaraldehyde crosslinked waste protein-based nanofiber nonwovens as an environmentally friendly wound dressing," React. Funct. Polym., vol. 172, no. February, p. 105203, 2022, doi: 10.1016/j.reactfunctpolym.2022.105203.

[18] Y. Z. Long, X. Yan, X. X. Wang, J. Zhang, and M. Yu, Electrospinning: The Setup and Procedure. Elsevier Inc., 2018. doi: 10.1016/B978-0-323-51270-1.00002-9.

[19] M. Sengor et al., "Core – shell PVA / gelatin nanofibrous scaffolds using co-solvent , aqueous electrospinning : Toward a green approach," J. Appl. Polym. Sci., vol. 46582, pp. 1–7, 2018, doi: 10.1002/app.46582.

[20] S. Wang et al., "Improvement in the Sustained-Release Performance of Electrospun Zein Nanofibers via Crosslinking Using Glutaraldehyde Vapors," Foods, vol. 13, no. 10, 2024, doi: 10.3390/foods13101583.

[21] Y. R. Chen et al., "Low-Molecular-Weight Heparin-Functionalized Chitosan-Chondroitin Sulfate Hydrogels for Controlled Release of TGF-β3 and in vitro Neocartilage Formation," 2019. doi: 10.3389/fchem.2019.00745.

★★★